

Article

A Molecular Interpretation on the Different Penetration Enhancement Effect of Borneol and Menthol towards 5-FU

Ran Wang ^{1,2,†}, Zhimin Wu ^{1,†}, Shufang Yang ^{1,2}, Shujuan Guo ¹,
Xingxing Dai ^{1,2}, Yanjiang Qiao ^{1,2,*} and Xinyuan Shi ^{1,2,*}

¹ Beijing University of Chinese Medicine, No.11 of North 3rd Ring East Road, Chaoyang District, Beijing 100029, China; wangran2017@sina.com (R.W.), WzMMzW@bucm.edu.cn (Z.W.), 18811795303@163.com (S.Y.), 18810820913@163.com (S.G.), jolly_1987@163.com (X.D.)

² Key Laboratory of TCM-information Engineer of State Administration of TCM, No.11 of North 3rd Ring East Road, Chaoyang District, Beijing 100029, China

[†] These authors contributed equally to this study.

* Correspondence: yjqiao@263.net (Y.Q.); shixinyuan01@163.com (X.S.); +86-10-8473-8621 (X.S. & Y.Q.)

Abstract: Borneol and menthol were two terpenes widely used as penetrate enhancer in transdermal drug delivery. To explore their penetration enhancement effect towards hydrophilic drug, 5-FU was selected as model drug. A method combined vitro permeation studies and coarse grain molecular dynamics was used to investigate their penetration enhancement effect towards 5-FU. As a result, although both borneol and menthol showed a penetration enhancement effect towards 5-FU, they differed a lot in the penetration enhancement mechanism, which was also thought to account for their different penetration enhancement effect. As for menthol, SC bilayer disrupting effect seemed to be its main mechanism. While for borneol, its mechanism seemed to be more complicated. Except for disrupting the SC bilayer, it could also increase the permeation of 5-FU by enhancing the diffusion rate of 5-FU or inducing the formation of transient pore. All of this enable us a molecular understanding of borneol and menthol's penetration enhancement effect towards hydrophilic drug, which might provide some guidance in the latter research and application.

Keywords: penetration enhancement effect; molecular mechanism; coarse grain molecular dynamics; menthol; borneol; 5-FU

1. Introduction

Transdermal drug delivery system (TDDs) has attracted considerable attention nowadays, as regards of its many potential advantages, including avoiding the first pass effect and improving the patient compliance [1]. All of this made TDDs a proper method for the administration of 5-FU, which was commonly used in the treatment of the treatment of colorectal cancer [2, 3]. However, because of the hydrophilic properties of 5-FU, it was very difficult for 5-FU to permeate through SC barrier. Varieties of ways have been tried to enhance the permeation of 5-FU, among this, the co-administration with penetration enhancer (PE) is the most widely accepted way. Especially the co-administration with natural products, such as terpenes [4, 5].

Terpene was a series of naturally occurring volatile oils that are composed of hydrocarbons and their oxygenated derivatives. It was appeared to be the clinically acceptable penetrate enhancers as indicated by its safety and high penetration enhancing effect [6, 7]. According to the former research done by Barry [8, 9], terpene was found to be able to enhance the penetration of 5-FU. Two important mechanisms were proposed in Barry's work, including complex formation and a form of facilitate transport. However, because of the limitation of detecting methods, a molecular explanation on the

partitioning of 5-FU from the aqueous region into the hydrocarbon interior of stratum corneum lipids was still lacked.

Molecular dynamics (MD) provide a convenient way to understand permeation processes and can yield important physical insights at molecular levels that could not be obtained from experiments because of associated time and length scale [10]. Further-more, a larger temporal and spatial scales could be explored during a simulation by altering molecular resolution, using an approach generally known as coarse-grained (CG) [11, 12]. Martini force field was the one of common CG force field developed by Marrink and his coworkers in 2007 [13], and it has been confirmed to be a powerful method in the research of bilayer system [14]. All of these make Martini CG MD a suitable method for us to get a molecular explanation on the penetration enhancement effect of terpene towards 5-FU.

Borneol and menthol were two terpenes widely used as penetrate enhancers, and their penetration enhancement effect have already been confirmed in the former research [15-18]. In this study, their penetration enhancement effect towards 5-FU were first investigated and compared, using a method combined vitro permeation studies and martini CG MD. As a result, a molecular explanation on the partitioning of 5-FU from the aqueous region into the hydrocarbon interior of stratum corneum lipids was hoped to gain through this study. What's more, a deeper understanding about the difference between borneol and menthol was also gotten. All of these will provide some guidance for the latter research and application of borneol and menthol.

2. Results and Discussion

2.1. *Vitro permeation studies on borneol and menthol's penetration enhancement effect towards 5-FU.*

A Franz diffusion experiment was implored to directly study the penetration enhancement effect of borneol and menthol towards 5-FU, and the penetration enhancing effect was assessed by comparison with the control group. What's more, in order to study the influence of PE concentration to the penetration enhancing effect, a series of concentrations of PE was investigated, including 0.1%, 0.2%, 0.3%, 0.4%, 0.5%, 1%, 2% and 3%. As a result, the transdermal drug permeation parameters were given in **Table 1**. Comparing with the control group, both borneol and menthol showed a penetration enhancing effect towards 5-FU at all the PE concentrations studied, and the penetration enhancement effect became stronger with the increasing of PE concentration. However, when the concentration of PE was larger than 0.5%, the influence of PE concentration on the penetration enhancement effect became small, and the penetration enhancement effect became stable. Such kind of phenomenon have been found in other research [19].

When it came to the differences between borneol and menthol, it was obviously that borneol gave a much stronger penetration enhancement effect towards 5-FU compared with that of menthol. According to the former QSPR research of terpene, hydrophobicity has a negative effect on the enhancement activity of terpenes towards 5-FU [20]. Since borneol(logP=2.71) gave a smaller than that of menthol(logP=3.2), so the results got in this study fit in well with the results got in QSPR research [21]. But when we put the logP value of borneol and menthol into the linear equation got in QSPR research, we found that the equation could not explain the huge difference between borneol and menthol. Therefore, in this study, instead of focusing on the logP value and other physiochemical properties of borneol and menthol, we tried to attribute their differences to their different penetration enhancement mechanism. According to the LPP theory [22, 23], two mechanisms were mainly discussed in this study to investigate borneol and menthol different penetration enhancement effect: 1. their different interaction with SC lipids; 2. their different influence on the partition and diffusion of 5-FU.

Table 1. Transdermal drug permeation parameters of borneol and menthol at different concentrations.

Concentration of PE	Borneol			Menthol		
	$J(\mu\text{g}/\text{cm}^2\cdot\text{h})$	$Q_{24}(\mu\text{g}/\text{cm}^2)$	ER	$J(\mu\text{g}/\text{cm}^2\cdot\text{h})$	$Q_{24}(\mu\text{g}/\text{cm}^2)$	ER
0.00%	0.82	20.45	1.00	-	-	-
0.10%	5.48	134.07	6.69	1.41	31.45	1.72
0.20%	6.40	160.36	7.80	2.13	46.95	2.60
0.30%	7.23	182.76	8.82	3.87	90.25	4.72
0.50%	12.51	299.43	15.26	3.85	96.94	4.70
1.00%	13.58	325.50	16.57	4.51	107.91	5.50
2.00%	14.19	342.11	17.31	4.05	96.71	4.94
3.00%	14.89	363.18	18.16	3.72	90.70	4.53

2.2. An investigation on borneol and menthol's influence on SC morphology using TEM experiment.

A TEM experiment was carried out to investigate the influence of borneol and menthol on the SC morphology, see **Figure 1**. Compared with the control group, the tightly packed lamellar structure was disrupted with the participating of borneol and menthol, and the disturbance became stronger with the increasing of PE concentration. Judged by the changes on the SC morphology, the differences between borneol and menthol was no distinct at a PE concentration below 2%. But when the PE concentration arrived at 3%, the difference between borneol and menthol on the SC morphology suddenly became distinct. As for the SC handle by 3% borneol, its morphology became vague, as if it has been solved. While for menthol, the SC structure stayed integral, although the disrupting effect became stronger compared with that at 2% PE concentration. Therefore, according to the results of TEM experiment, both borneol and menthol showed a disrupting effect on the SC morphology. And the differences between their disrupting effect was not distinct until the PE concentration was at 3%, at which borneol showed a disrupting effect much stronger than that of menthol.

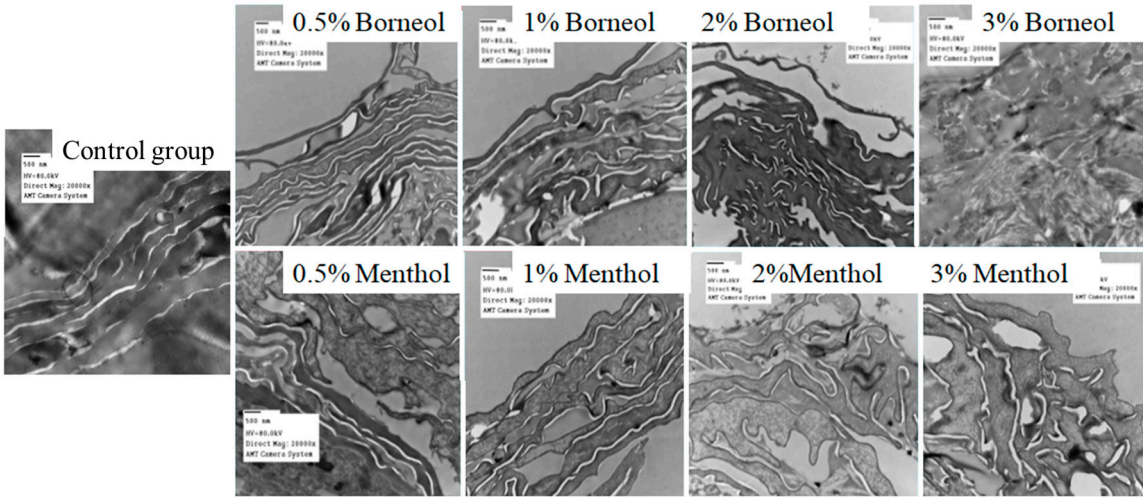


Figure 1. Transmission electron micrographs of 24h drug treated epidermis. The direct magnification of all graphs is 20000 at 80kV.

2.3. An investigation on borneol and menthol's influence to SC morphology using CG MD.

In this study, borneol and menthol's influence on the SC morphology were also investigated using a method of CG MD. For the better representation of SC bilayer, a mixed ceramide lipid model is used in this assay, which is composed of heterogeneous mixture of ceramides (CER), cholesterol (CHOL) and free fatty acid (FFA) in a ratio of 2: 2: 1. Besides, a series concentration of borneol and menthol were also studied to investigate the influence of PE concentration to the penetration

enhancing effect. It's worth to be noted that because of different study scale between vitro permeation study and CG MD, the concentration of PE might differ from each other in number.

The final bilayer morphology handled by borneol and menthol was compared at first to get a general understanding of their influence on SC bilayer, see **Figure 2**. Although, compared with the initial SC bilayer in **Figure 7b**, both borneol and menthol could induce a slight curvature on SC bilayer at PE concentration below 7%, their differences was not distinct. However, when the PE concentration arrived 10%, the bilayer handled by borneol became chaos and the bilayer structure was almost destroyed; while for menthol, although the curvature became stronger, its bilayer structure stayed integral. Thus, borneol showed a stronger influence on the SC bilayer morphology at PE concentration beyond 10%.

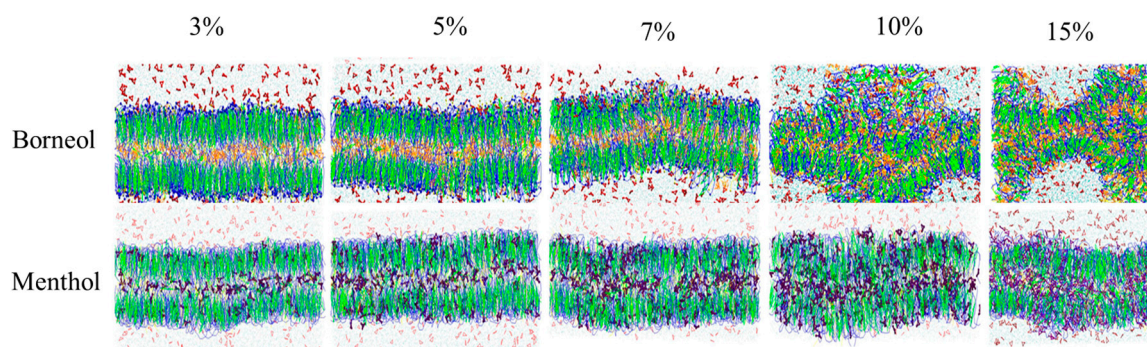


Figure 2. The final bilayer morphology handled by borneol (top) and menthol (blow) at different PE concentrations.

Further study had been carried out on the distribution of borneol and menthol along the z axis to investigate their influence on the SC morphology. Taking the results of 7% PE concentration as an example, see **Figure 3**. Except the density distribution of borneol and menthol (plotted by solid line), 4 other components were also plotted by dotted line, including hydrophilic, hydrophobic groups of CER, solvent and 5-FU. They were used to better clarify the relative location of borneol and menthol in the bilayer, and their density was indicated using the first axis at the left side of the density distribution curve. Because of the low-density distribution of borneol and menthol in the bilayer, their density was indicated using the second axis at the right side of the density distribution curve.

There were three peaks in the density distribution curve for both borneol (yellow) and menthol (purple). The highest one located at the same position with the hydrophobic group of CER, the other two peaks located just under the hydrophilic group of CER. Another thing could be observed in the density distribution curve was that, borneol gave a lower-density distribution in the bilayer center and a higher-density distribution under the hydrophilic group of CER. Since borneol and menthol both contained a hydroxyl group, they were supposed to interact with hydrophilic group of CER through H-bond, and such kind of interaction was thought to show an impacted on the SC bilayer morphology [15, 24]. Therefore, the higher distribution of borneol under the hydrophilic group of CER lipids might have indicated its stronger interaction with the hydrophilic group of CER, which was also thought to be related with borneol's stronger influence on the SC bilayer morphology at a PE concentration larger than 10% [25].

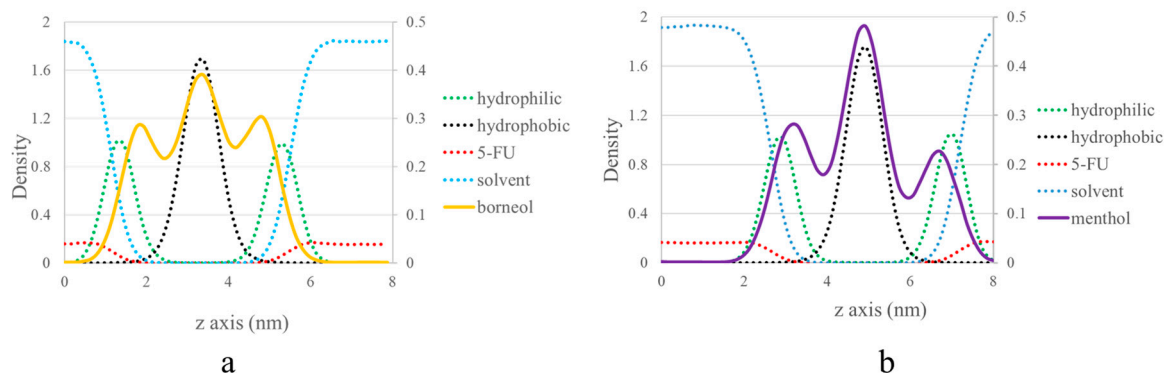


Figure 3. Density distribution of borneol (a) and menthol (b) along the z axis at 7% PE concentration. The other four components including hydrophilic group of CER(hydrophilic), hydrophobic group of CER(hydrophobic), solvent and 5-FU, were displayed in dotted line to better clarify the relative location of borneol and menthol, and their density were indicated using the first axis at the left side. Since borneol and menthol showed a low-density distribution in the bilayer, their density were indicated using the second axis at the right side.

Combine the results of this part and the TEM experiment, conclusions could be made that: both borneol and menthol showed a strong interaction with the hydrophilic group of CER, and this was thought to show an influence on the bilayer structure. As indicated by the higher-density distribution of borneol under the hydrophilic group of CER, the interaction between borneol and the head group of SC lipids was thought to be stronger than that of menthol, which means borneol might own a stronger influence on the SC bilayer structure. Besides, the influence of borneol and menthol on the SC bilayer structure was also affected by the PE concentration, so the differences between borneol and menthol in inducing the changes on SC morphology were not distinct at a relative low PE concentration.

2.4. An investigation on borneol and menthol's influence on the diffusion of 5-FU using CG MD.

To explore the influence of borneol and menthol on the diffusion of 5-FU, the diffusion constant of 5-FU along the axis of z (perpendicular to the bilayer surface) was calculated using the method described in the 3.1.3. See **Figure 4**. As for menthol, no distinct changes in diffusion constant could be observed with the increasing of PE concentration, thus menthol showed little influence on the diffusion of 5-FU. While for borneol, the diffusion constant of 5-FU went up quickly with the participating of borneol, which means 5-FU would get more probability to permeate into the bilayer under the help of borneol, and it was thought to be account for borneol's stronger penetration enhancement effect from some extent. Besides, it was worth to note that, although the diffusion constant kept going up with the increasing of PE concentration, the rate of increasing was very small, which might indicate that there was some other mechanism that should be account for borneol's stronger penetration enhancement effect at a PE concentration higher than 10%.

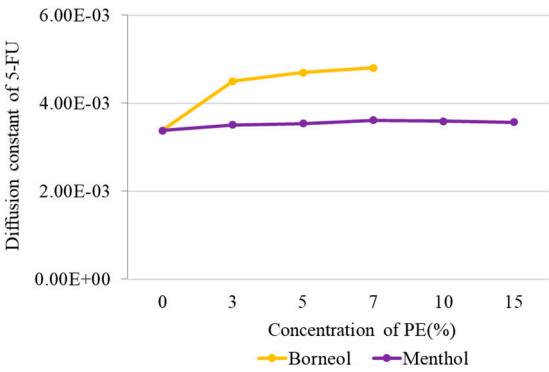


Figure 4. Diffusion constant of 5-FU along the z axis at different PE concentration. As for borneol, because of the destroy of membrane structure, the diffusion constant of 5-F has lost its original mining in evaluating the penetration enhancement effect, so it was vacancy at a borneol concentration larger than 10%.

2. 5. A molecular explanation on the partitioning of 5-FU from the aqueous region into the hydrocarbon interior of stratum corneum lipids

Based on the discussion before, a deeper understanding was got on borneol and menthol’s penetration enhancement effect towards 5-FU. But from some extent, our CG MD study was always limited by the PE concentration, that was because we were not familiar with their penetration enhancement mechanism at a PE concentration higher than 10%. So, at this part, efforts were made to investigate the underlying reason of borneol’s stronger penetration enhancement effect at a PE concentration higher than 10%. As a result, a phenomenon was thought to largely affect the permeation of 5-FU. Taking the phenomenon observed at a 15% borneol concentration as an example, see **Figure 5a**. From left to right, more and more CER headgroups were observed in the bilayer center. A path consisted of CER headgroups was formed, and this path pointed directly into the bilayer center. Because of the hydrophilic property of CER headgroups, the path was thought to largely facilitate the permeation of 5-FU. Such kind of path have also been found in former research, and it was called transient pore [26].

Fortunately, the permeation of one 5-FU molecular into the bilayer center was also observed in the molecular trajectory of 15% borneol concentration. As can be seen from **Figure 5b**, the 5-FU molecular penetrated from a position ($z=5.70\text{nm}$) outside the bilayer into a position ($z=3.96\text{nm}$) near the bilayer center under the help of transient pore.

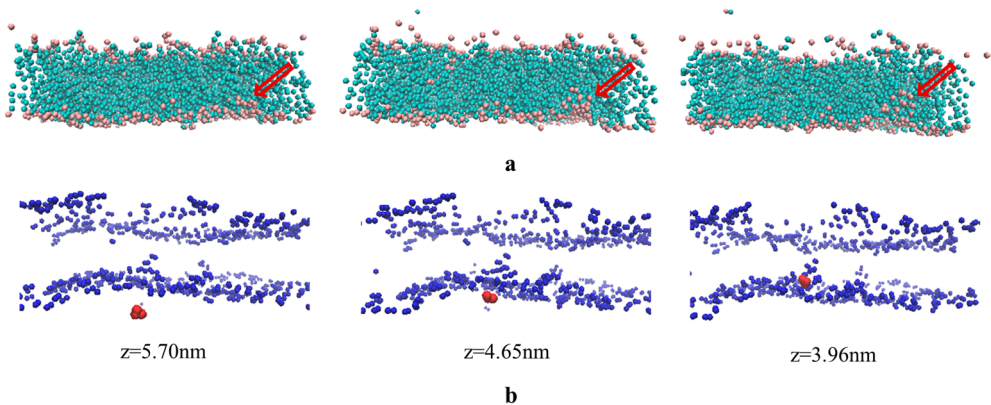


Figure 5. The formation of transient pore and diffusion of 5-FU from the aqueous region into the hydrocarbon interior of stratum corneum lipids. a). The aggregating of CER headgroups in the bilayer center and the formation of transient pore. For the better representation transient pore, the other components were set implicit, except CER (pink for headgroups and light green for tail groups). b). The diffusion of 5-FU from the aqueous region into the hydrocarbon interior of stratum

corneum lipids the aggregating of CER molecular in bilayer center, and their z axis coordinate was given blow. For the better clarification, only headgroups of CER (blue) and 5-FU (red) were displayed in the picture.

Although the formation of transient pore had also been observed in other groups, they differ a lot from each other, especially in the time that transient pore lasted. Considering the importance of transient pore for the permeation of 5-FU, the time that transient pore lasted was used to evaluate the penetration enhancement effect of borneol and menthol, see **Figure 6**. Both PE type and PE concentration showed a great influence on the time that transient pore lasted. The transient pore was not observed until a PE concentration was beyond 3%. Then with the increasing of PE concentration, transient pore came into being and the time that transient pore lasted was also prolonged. What's more, the CER aggregates induced by borneol tended to last much longer than that of menthol, especially at a PE concentration larger than 10%. There was no doubt that the long opening time of transient pore would largely facilitate the permeation of 5-FU. Knowing this, it will not be hard to understand borneol's stronger penetration enhancement effect towards 5-FU at a PE concentration beyond 10%.

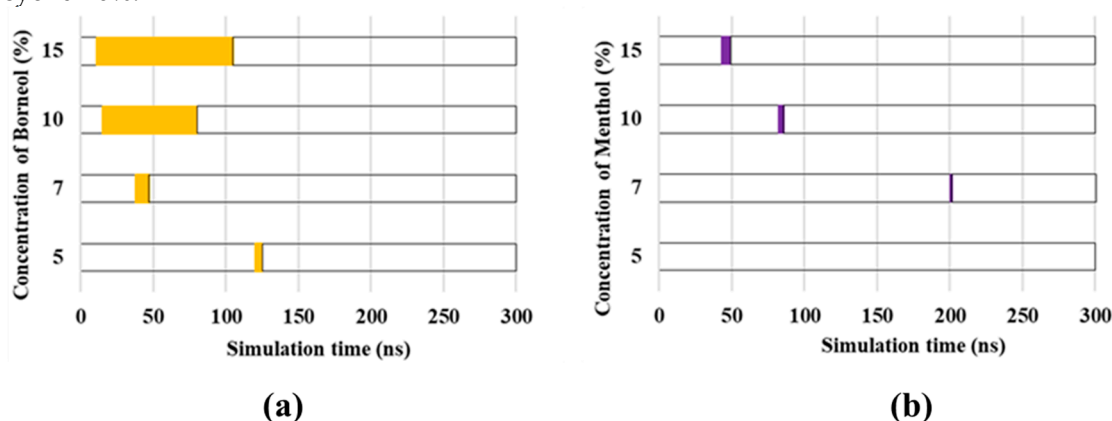


Figure 6. Molecular trajectory of borneol (a) and menthol (b) at different PE concentration during the whole 300 ns. The observation of the transient pore formation was painted in purple and yellow, from the time transient pore was observed and the time transient pore disappeared.

3. Materials and Methods

3.1. CG-MD simulation

3.1.1. CG molecular models and initial structures

This assay mainly involves eight molecules, 5-FU, borneol, menthol, CER, CHOL, FFA, PG and water. The parameter files of the CG models of CER, CHOL, FFA, PG and water are available in the Martini website, and the CG model of 5-FU, borneol, and menthol were developed according to the CG recipe published in the Martini website. CG model of borneol and menthol have already been validated in the former research of our group [14, 27]. As for the CG model of 5-FU, the whole parameters and verification progress were shown in the Supplementary Materials.

The bilayer model of SC in this study is composed of CER, CHOL and FFA in a 2:2:1 molar ratio, whose properties have been validated by Das and his coworkers in 2009 [28]. The bilayer systems with different menthol concentrations in water are built using the Packmol package [29] and figures depicting lipid molecules are generated with Visual Molecular Dynamics (VMD) [30]. The coarse grain model of main molecular and the morphology of blank bilayer are shown in **Figure 7**.

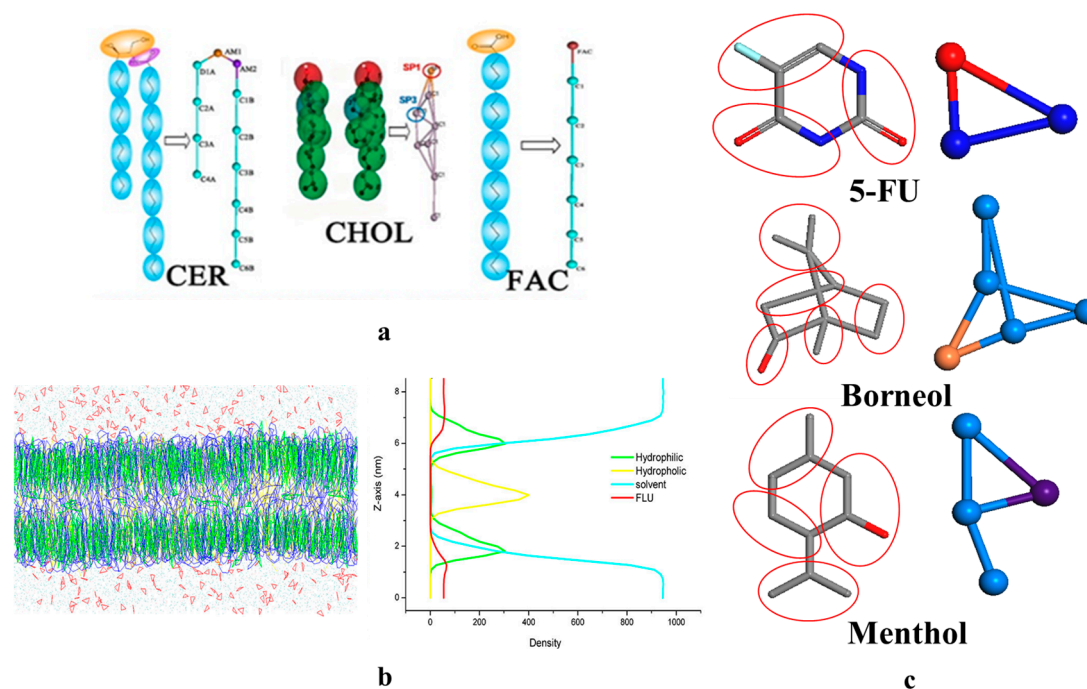


Figure 7. CG mapping for 6 main compounds used in this study and the initial bilayer morphology. a). CG mapping for the main bilayer components, including ceramides(CER), cholesterol(CHOL), and free fatty acid(FFA), they were download from Martini website. b). CG mapping for borneol(BO), menthol(MEN) and fluorouracil(FLU), they were build and optimized by our group. c). The morphology of blank membrane composed of heterogeneous mixture of long chain ceramides (CER), cholesterol (CHOL) and free fatty acid (FFA) in a ratio of 2: 2: 1, together with its distribution of four components along the z axis.

3.1.2. Simulation Details

The simulation was conducted with the GRONINGEN Machine for Chemical Simulation (GROMACS, Ver 4.6.3). Prior to simulation, the system was relaxed through energy minimization (EM) using the steepest descent algorithm through which the potential energy was descended to be negative on the order of 105-106 and the maximum force was adjusted to less than 80 kJmol⁻¹. Standard simulation parameters associated with the MARTINI force field were used. The temperature was regularized constantly by using Berendsen Temperature coupling with a time constant of 1.0 ps, and the pressure was controlled by Berendsen Barostat and semi-isotropic pressure coupling with a constant of 3.0 ps and compressibility of 4.5×10⁻⁴/bar. The neighbor searching algorithm was implemented and the cut-off distance was set as 1.4 nm. The method was shifted and the cut-off length was picked at 1.2 nm for both the Van der Waals and electrostatic potentials. A time step was preset as 20 fs, and finally, trajectory data with 300 ns in total was gained.

3.1.3. Important parameters

The main important parameters used in coarse grain molecular dynamics were diffusion constant D (nm²/ps).

we quantified the phospholipid dynamics by computing the 5-FU molecule diffusion coefficient along the axis of z, D_{5-FU}, which was extracted from the Einstein relation:

$$\Delta r(t)^2 = \frac{1}{N_{5-FU}} \sum_{i=1}^{N_{5-FU}} (r_i(t) - r_i(0))^2 \quad (2)$$

$$D_{5-FU} = \lim_{t \rightarrow \infty} \frac{1}{4t} (\Delta r(t)^2) \quad (3)$$

where $\Delta r(t)^2$ is the average mean square displacement of 5-FU molecular along the axis of Z at time t. In this work, we employed 3000 configurations across 300 ns simulation time to perform the calculation over all 5-FU molecular.

3.2. *In vitro* Permeation Studies

3.2.1. *Materials and Reagents*

Borneol, menthol and 5-FU (purity > 98%) were purchased from the National Institutes for Food and Drug Control (Beijing, China). Phosphate buffer saline (PBS, pH 7.2–7.4, 0.01M) was purchased from Beijing Solarbio Science and Technology Co., Ltd. Glutaraldehyde (2.5%) was obtained from Biotopped Life Sciences. Methanol of HPLC grade were supplied by Thermo Fisher Scientific (China). 1,2-propanediol (PG), ether and sodium chloride were purchased from Beijing Chemical Works.

3.2.2. *Preparation of samples*

Terpene in co-solvent systems: 20/80 (v/v) water/propanediol, were used for the delivery of 5-FU [31]. 5-FU was first dissolved in the co-solvent system. Then the 5-FU solution was used as solvent to prepare different concentration of borneol and menthol. The concentrations of borneol and menthol were 0.1%, 0.2%, 0.3%, 0.4%, 0.5%, 1.0%, 2.0% and 3.0%.

3.2.3. *Preparation of skin*

The skin was excised from male Sprague-Dawley rats (five weeks of age, (200 ± 10g), supplied by Sibeifu Laboratory Animal Technology Co., Ltd). The rats were anesthetized with excess ether inhalation, and the abdominal skin was excised after removing hair with an animal hair clipper. After removing the fat and subcutaneous tissue, the skin was cleaned with ultrapure water and 0.9% sodium chloride. All animal experimental procedures were conducted in conformity with institutional guidelines for the care and use of laboratory animals.

3.2.4. *Skin Permeation*

Freshly excised rats' corneas were immediately mounted over the modified Franz-type vertical diffusion chambers. Blank 80% propanediol (15ml) was added to the endothelial side and maintained at 32°C under mixed conditions with a 2-ml donor solution with a constant magnetic stirring rotating at the speed of 350 rpm. The available corneal area for diffusion was 1.23 cm². Samples of 1.5 ml were taken from the endothelial side and replaced with an equal volume of blank 80% propanediol at the time points: 2, 4, 6, 8, 10, 12, and 24 hours. All of the solution samples were filtered through a 0.45-μm Millipore filter (Jin Teng) and stored at 4°C.

3.2.5. *Instrumentation and Chromatographic Conditions*

The quantitative determination of 5-FU was performed with an HPLC system (Agilent 1100, Agilent, USA.) using methanol-water (5:95 v/v) in the mobile phase at a flow rate of 1.0 ml/min. The injection volume was 10 μl. A Waters Xbridge C18 column (250 × 4.6 mm, 5 μm, Waters, USA.) was used. The UV detector wavelength was set at 266 nm and the column temperature was maintained at 35 °C.

3.2.6. *Transmission Electron Microscope (TEM) Studies*

The skin samples were fixed instantaneously with 2.5% glutaraldehyde after permeation. Samples were then post-fixed in 1% OsO₄ and dehydrated in a graded series of acetone. The samples were subsequently embedded in a low-viscosity epon-epoxy mixture and sectioned. Thin sections

were double stained with uranyl acetate and lead citrate and then examined on a transmission electron microscope (JEOL JEM-1230, Japan) operated at 80 kV.

3.2.7. Important parameters

The main parameters used in this paper to assess the permeation enhancing effect were: the cumulative amount Q_n ($\mu\text{g}/\text{cm}^2$), the permeability constant J ($\mu\text{g}/\text{cm}^2\cdot\text{h}$) and the enhancement ratio ER.

The quantity of drugs that permeated through SC is presented as cumulative amount Q_n ($\mu\text{g}/\text{cm}^2$) and is calculated using the following formula:

$$Q_n = \frac{C_n \times V_r + \sum_{i=1}^{n-1} C_i \times V_i}{A} \quad (4)$$

where C_n is the drug concentration of the receptor medium at each sampling time, C_i is the drug concentration at i th sampling point, V_r and V_i were the volumes of receptor solutions and samplings, respectively, and A was the effective diffusion area of skin.

The zero-order permeating kinetics equation (Q - t) is obtained by regressing the cumulative amount on time:

$$Q = Jt + BQ = Jt + B \quad (5)$$

where the slope J ($\mu\text{g}/\text{cm}^2\cdot\text{h}$) is the permeability constant.

The permeability coefficient of drugs is related to permeability coefficient K_p (cm/h) using the following formula:

$$K_p = J/C_0 \quad K_{pe} = J/C_0 \quad (6)$$

where C_0 ($\mu\text{g}/\text{mL}$) is the initial concentration of drug.

The overall potency of PE is expressed as enhancement ratio (ER), a ratio of the K_p value before and after enhancer treatment:

$$ER = K_{pe} / K_p \quad (7)$$

where K_{pe} is the K_p value after treatment.

4. Conclusions

In this study, the results from vitro permeation study and CG MD got along well with each other, both confirmed borneol and menthol's penetration enhancement effect towards 5-FU. What's more important was that the results in CG MD gave a molecular understanding of borneol and menthol's different penetration enhancement effect towards 5-FU. As for menthol, SC bilayer disrupting effect seemed to be the single mechanism of its penetration enhancement effect. While for borneol, its mechanism tended to be more complicated, except for the SC bilayer disrupting effect, it could also enhance the permeation of 5-FU by increasing its diffusion constant or the forming of transient pore. It was the multiple penetration enhancement mechanism that lead to borneol's stronger penetration enhancement effect. Based on the results of this study, a deeper understanding of borneol and menthol's penetration enhancement effect towards hydrophilic drugs was gotten, which might provide some guidance for the future research and application.

Supplementary Materials: The following are available online at www.mdpi.com/link

Acknowledgments: This work was financially supported by the National Natural Science Foundation of China (81473364), Beijing Natural Science Foundation (7162122), and Excellent Talents Training Subsidy Scheme of Beijing (2013D009999000003).

Author Contributions: Xinyuan Shi and Yanjiang Qiao designed the experiments, revised the manuscript and approved the final version; Ran Wang and Wu Zhimin performed the experiments, acquired and analyzed the data, and drafted the manuscript; Shufang Yang, Xingxing Dai and Shujuan Guo provided some technical guidance, helped perform the analysis with constructive discussions, and revised the manuscript.

364 **Conflicts of Interest:** The authors declare no conflict of interest.

365 References

- 366 1. Subedi, R.K.; Oh, S.Y.; Chun, M-K.; Choi, H-K. Recent advances in transdermal drug delivery. *Arch Pharm*
367 *Res.* **2010**, *33*, 339-351. doi:10.1007/s12272-010-0301-7.
- 368 2. Chionh, F.; Campbell, A.; Sukumaran, S.; Price, T.; Tebbutt, N. Oral versus intravenous fluoropyrimidines
369 for colorectal cancer. *Cochrane Db Syst Rev.* **2017**, *7*, CD008398.
- 370 3. Sawai, Y.; Yamaoka, K.; Ito, T.; Nakagawa, T. (1997). Simultaneous evaluation of intestinal absorption and
371 hepatic extraction of 5-fluorouracil using portal-systemic concentration difference by short-period double
372 dosing in a single conscious rat. *Biol Pharm Bull.* **1997**, *20*, 1313-1319.
- 373 4. Singh, B.N.; Singh, R.B.; Singh, J. Effects of ionization and penetration enhancers on the transdermal
374 delivery of 5-fluorouracil through excised human stratum corneum. *Int J Pharm.* **2005**, *298*, 98-107. doi:
375 10.1016/j.ijpharm.2005.04.004.
- 376 5. Xie, F.; Chai, J.K.; Hu, Q.; Yu, Y.H.; Ma, L.; Liu, L.Y.; Zhang, X.L.; Li, B.L.; Zhang, D.H. Transdermal
377 permeation of drugs with differing lipophilicity: effect of penetration enhancer camphor. *Int J Pharm.* **2016**,
378 *507*, 90-101. doi:10.1016/j.ijpharm.2016.05.004.
- 379 6. Patil, U.K.; Saraogi, R. Natural products as potential drug permeation enhancer in transdermal drug
380 delivery system. *Arch Dermatol Res.* **2014**, *306*, 419-426. doi:10.1007/s00403-014-1445-y.
- 381 7. Lane, M.E. Skin penetration enhancers. *Int J Pharm.* **2013**, *447*, 12-21. doi:10.1016/j.ijpharm.2013.02.040.
- 382 8. Moghimi, H.R.; Williams, A.C.; Barry, B.W. Enhancement by Terpenes of 5-Fluorouracil Permeation
383 through the Stratum Corneum: Model Solvent Approach. *J. Pharm. Pharmacol.* **1998**, *50*, 955-964.
- 384 9. Cornwell, P.A.; Barry, B.W. Sesquiterpene Components of Volatile Oils as Skin Penetration Enhancers for
385 the Hydrophilic Permeant 5-Fluorouracil. *J. Pharm. Pharmacol.* **1994**, *46*, 261-269.
- 386 10. Notman, R.; Anwar, J. Breaching the skin barrier - Insights from molecular simulation of model
387 membranes. *Adv Drug Deliv Rev.* **2013**, *65*, 237-250. doi:10.1016/j.addr.2012.02.011.
- 388 11. Otto, D.P.; Villiers, M.M. De. The Experimental Evaluation and Molecular Dynamics Simulation of a
389 Heat-Enhanced Transdermal Delivery System. *AAPS Pharm Sci Tech.* **2013**, *14*, 111-121.
390 doi:10.1208/s12249-012-9900-6.
- 391 12. Lopez, C.A.; Uusitalo, J.J.; Jong, D.H.; De, Gopal, S.M.; Periole, X. The power of coarse graining in
392 biomolecular simulations. *Wiley Interdiscip Rev Comput Mol Sci.* **2014**, *4*, 225-248. doi:10.1002/wcms.1169.
- 393 13. Marrink, S.J.; Risselada, H.J.; Yefimov, S.; Tieleman, D.P. De, Vries, A.H. The MARTINI force field: Coarse
394 grained model for biomolecular simulations. *J Phys Chem B.* **2007**, *111*, 7812-7824. doi:10.1021/jp071097f.
- 395 14. Dai, X.; Yin, Q.; Wan, G.; Wang, R.; Shi, X. Effects of Concentrations on the Transdermal Permeation
396 Enhancing Mechanisms of Borneol: A Coarse-Grained Molecular Dynamics Simulation on Mixed-Bilayer
397 Membranes. *Int. J. Mol. Sci.* **2016**, *17*, 1349. doi:10.3390/ijms17081349.
- 398 15. Chen, Y.; Wang, J.; Cun, D.; et al. Effect of unsaturated menthol analogues on the in vitro penetration of
399 5-fluorouracil through rat skin. *Int J Pharm.* **2013**, *443*, 120-127. doi:10.1016/j.ijpharm.2013.01.015.
- 400 16. Liu, J.; Fu, S.; Wei, N.; Hou, Y.; Zhang, X.; Cui, H. The effects of combined menthol and borneol on
401 fluconazole permeation through the cornea ex vivo. *Eur J Pharmacol.* **2012**, *688*, 1-5.
402 doi:10.1016/j.ejphar.2011.12.007.
- 403 17. Lan, Y.; Wang, J.; Li, H.; et al. Effect of menthone and related compounds on skin permeation of drugs
404 with different lipophilicity and molecular organization of stratum corneum lipids. *Pharm Dev Technol.*
405 **2015**, *0*, 1-10. doi:10.3109/10837450.2015.1011660.
- 406 18. Yi, Q-F.; Yan, J.; Tang, S-Y.; Huang, H.; Kang, L-Y. Effect of borneol on the transdermal permeation of
407 drugs with differing lipophilicity and molecular organization of stratum corneum lipids. *Drug Dev Ind*
408 *Pharm.* **2016**, *42*, 1086-1093. doi:10.3109/03639045.2015.1107095.
- 409 19. Ahad, A.; Aqil, M.; Ali, A. The application of anethole, menthone, and eugenol in transdermal penetration
410 of valsartan: Enhancement and mechanistic investigation. *Pharm Biol.* **2015**, *54*, 1-10.
411 doi:10.3109/13880209.2015.1100639.
- 412 20. Ghafourian, T.; Zandasrar, P.; Hamishekar, H.; Nokhodchi, A. The effect of penetration enhancers on drug
413 delivery through skin: A QSAR study. *J Control Release.* **2004**, *99*, 113-125. doi:10.1016/j.jconrel.2004.06.010.
- 414 21. Chen, J.; Jiang, Q.D.; Chai, Y.P.; Zhang, H.; Peng, P.; Yang, X.X.; Natural terpenes as penetration enhancers
415 for transdermal drug delivery. *Molecules.* **2016**, *21*, 1-22. doi:10.3390/molecules21121709.

22. Sapra, B.; Jain, S.; Tiwary, A.K. Percutaneous Permeation Enhancement by Terpenes: Mechanistic View. *AAPS J.* **2008**, *10*, 120-132. doi:10.1208/s12248-008-9012-0.
23. Narishetty, S.T.K.; Panchagnula, R. Transdermal delivery of zidovudine: Effect of terpenes and their mechanism of action. *J Control Release.* **2004**, *95*, 367-379. doi:10.1016/j.jconrel.2003.11.022.
24. Jain, A.K.; Thomas, N.S.; Panchagnula, R. Transdermal drug delivery of imipramine hydrochloride. i. effect of terpenes. *J Control Release.* **2002**, *79*, 93-101.
25. Zhu, W.; Xiong, L.; Peng, J.; Deng, X.; Gao, J.; Li, C.M. Structure-dependent membrane perturbing potency of four proanthocyanidin dimers on 3T3-L1 preadipocytes. *J Agr Food Chem.* **2016**, *64*, 7022-7032.
26. Gurtovenko, A. a.; Anwar, J. Modulating the structure and properties of cell membranes: the molecular mechanism of action of dimethyl sulfoxide. *J Phys Chem B.* **2007**, *111*, 10453-10460. doi:10.1021/jp073113e.
27. Wan, G.; Dai, X.; Yin, Q.; Shi, X.; Qiao, Y. Interaction of menthol with mixed-lipid bilayer of stratum corneum: A coarse-grained simulation study. *J Mol Graph Model.* **2015**, *60*, 98-107. doi:10.1016/j.jmgm.2015.06.005.
28. Das, C.; Noro, M.G.; Olmsted, P.D. Simulation Studies of Stratum Corneum Lipid Mixtures. *Biophys J.* **2009**, *97*, 1941-1951. doi:10.1016/j.bpj.2009.06.054.
29. Martínez, L.; Andrade, R.; Birgin, E.G.; Martínez, J.M. Software News and Update Packmol: A Package for Building Initial Configurations. **2009**. doi:10.1002/jcc.
30. Humphrey, W.; Dalke, A.; Schulten, K. VMD: Visual Molecular Dynamics. **1996**, *7855*, 33-38.
31. Yamane, M.A.; Williams, A.C.; Barry, B.W. Terpene Penetration Enhancers in Propylene Glycol/water Co-solvent Systems: Effectiveness and Mechanism of Action. *J. Pharm. Pharmacol.* **1995**, *47*, 978-989.